

Supporting Information

for

Effect of Conjugated Length on the Properties of Fused Perylene
Diimides with variable Isoindigos

Yaping Yu, Ning Xue, Chengyi Xiao, Mahesh Kumar Ravva, Yanjun Guo, Liyun Wu, Lei Zhang,
Zhengke Li, Wan Yue, Zhaohui Wang

Table of contents

1. Absorption spectra and CV of isolated PDI and IID.....	S2
2. DFT results.....	S2
3. DPVs.....	S9
4. OFET device fabrication and characterization.....	S9
5. Experimental details.....	S11
6. NMR Spectra of compounds.....	S14
7. HRMS spectra.....	S18
8. References.....	S22

1. Absorption spectra and CV of isolated PDI and IID

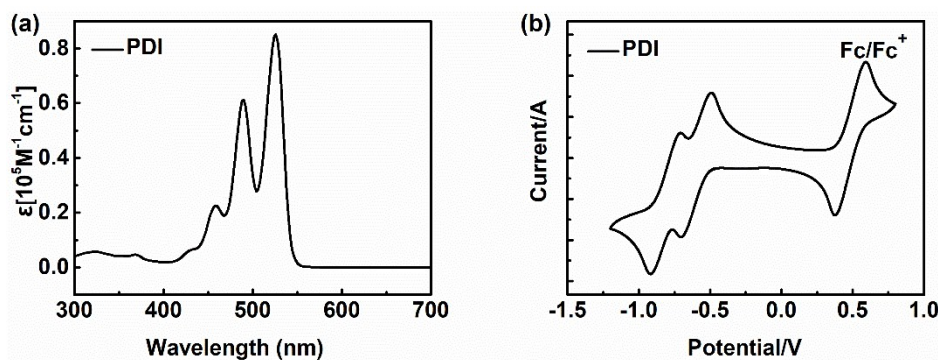


Figure S1: The absorption spectra of isolated **PDI** in chloroform solution (a) and reductive cyclic voltammetry in CH_2Cl_2 solution (b).

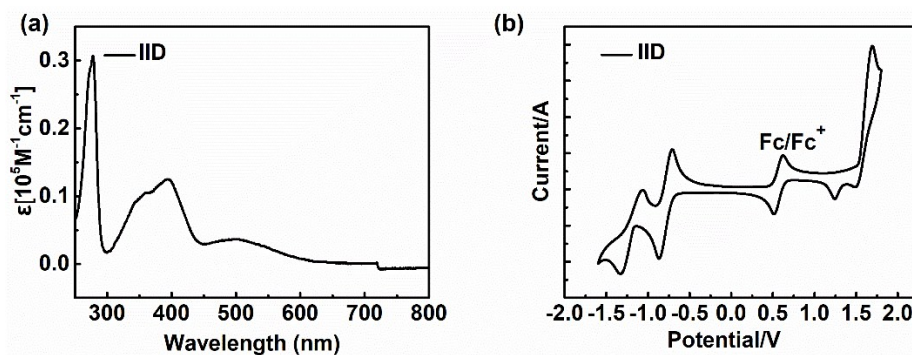


Figure S2: The absorption spectra of isolated **IID** in chloroform solution (a) and Reductive cyclic voltammetry in CH_2Cl_2 solution (b).

2. DFT results.

Table S1: Calculated optical properties of various molecules as determined with TDDFT at the PCM (chloroform)-OT- ω B97XD/6-31G** level of theory.

Compound	E(S ₁)/nm	E(S ₃)/nm	E(S ₅)/nm	E(S ₇)/nm	E(S ₉)/nm	E(S ₁₂)/nm
PDI	525					
IID	516	395	-	250		
PDI-IID	556	-	475	-	367	
PDI-IID-PDI	580		516	489	470	
PDI-BDOPV-PDI	671					457
PDI-DPN-PDI	850					570

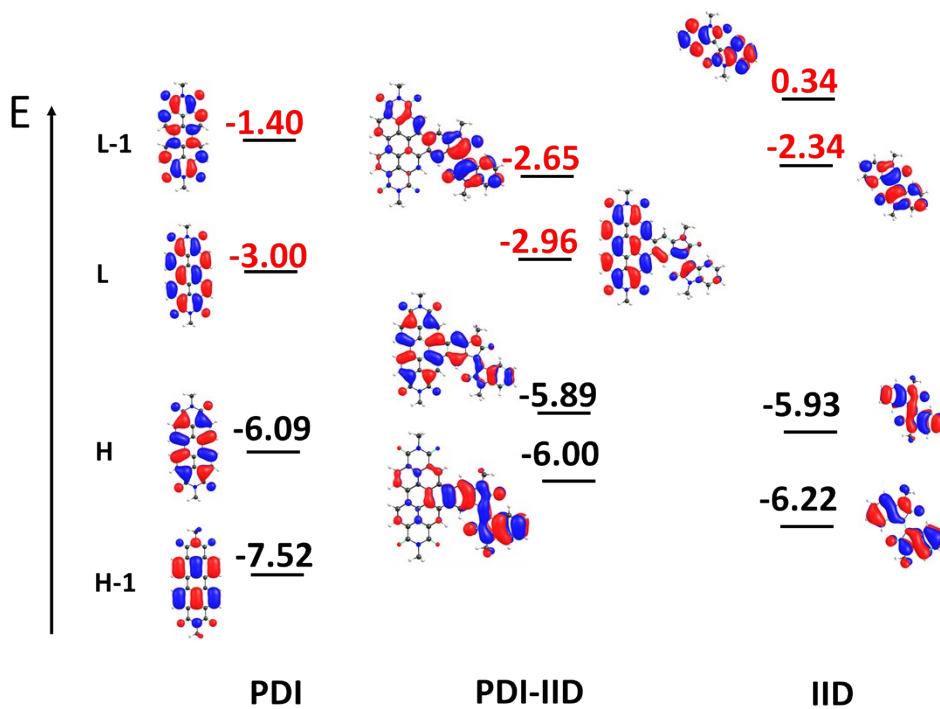


Figure S3: Pictorial representation of one-electron wavefunctions of isolated **PDI**, **IID**, and fused **PDI-IID** molecules, calculated at PCM (chloroform)-OT- ω B97XD/6-31G(d,p) level of theory. All values in eV.

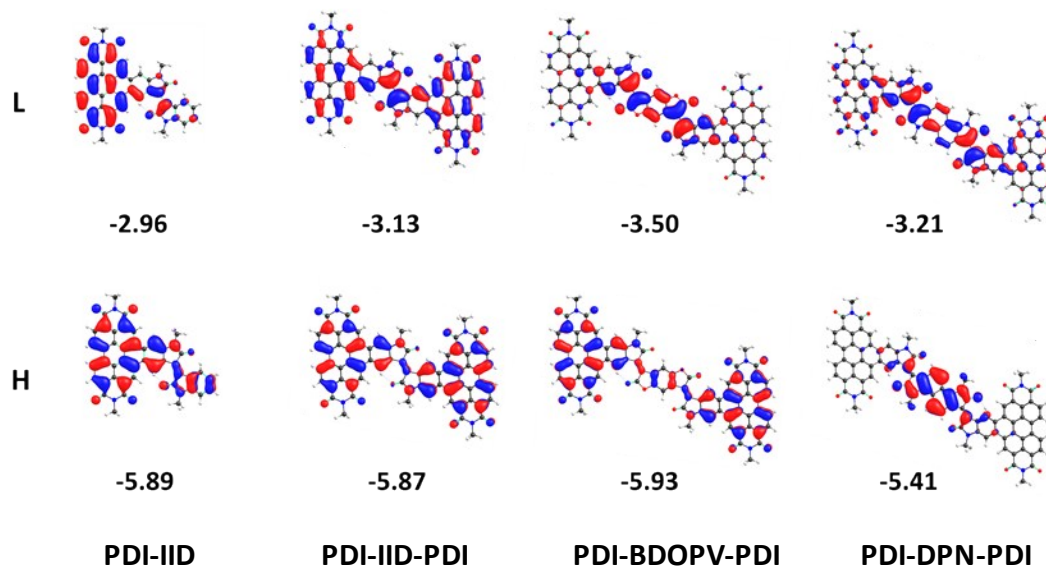


Figure S4: Pictorial representation of one-electron wavefunctions of **PDI-IID**, **PDI-IID-PDI**, **PDI-BDOPV-PDI**, and **PDI-DPN-PDI** molecules, calculated at PCM (chloroform)-OT- ω B97XD/6-31G(d,p) level of theory. All values in eV.

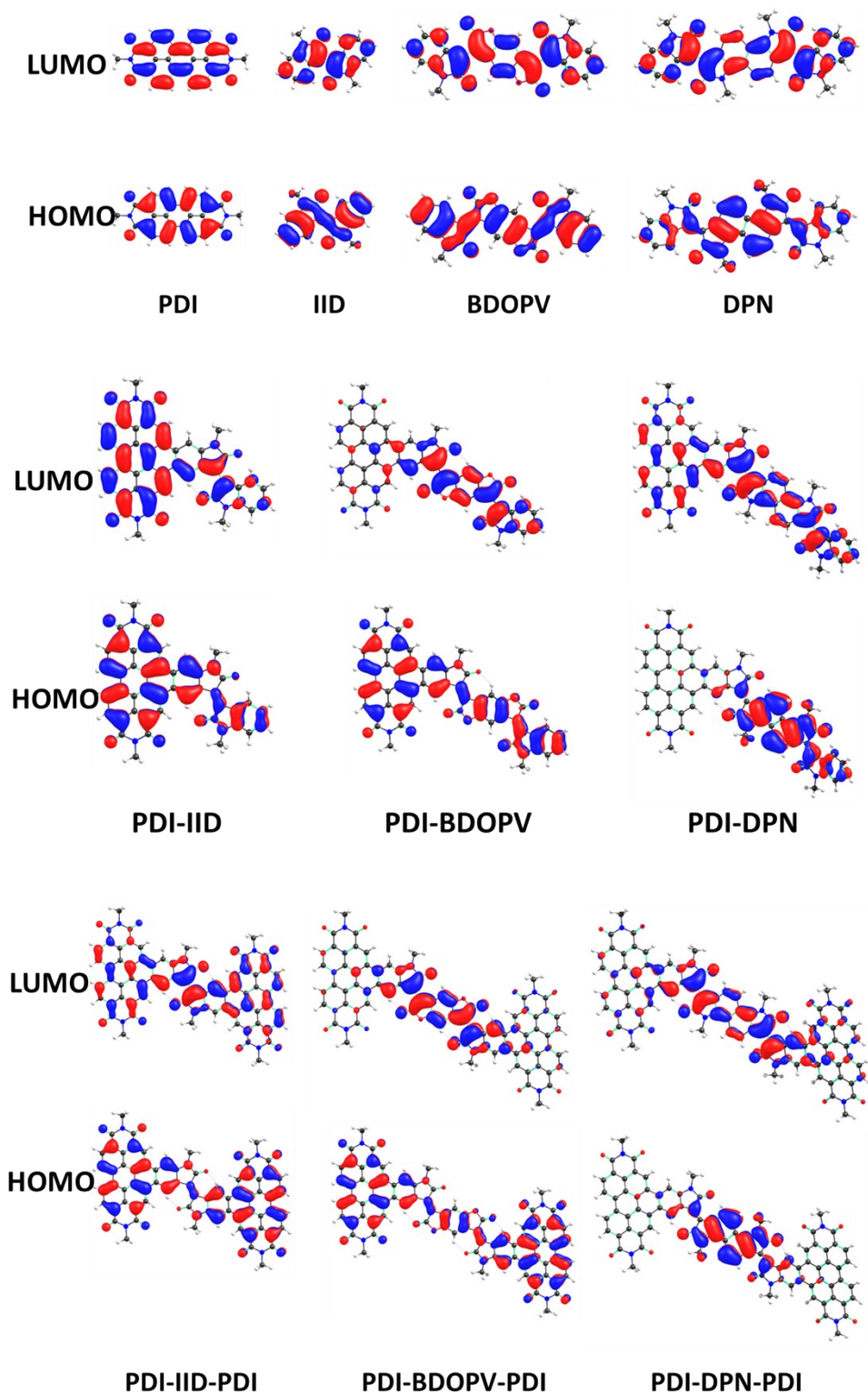


Figure S5: Pictorial representation of one-electron wavefunctions of isolated **PDI**, **IID**, **BDOPV**, **DPN** and fused **PDI-IID**, **PDI-BDOPV**, **PDI-DPN**, **PDI-IID-PDI**, **PDI-BDOPV-PDI**, **PDI-DPN-PDI** molecules, calculated at B3LYP/6-31G(d,p) level of

theory.

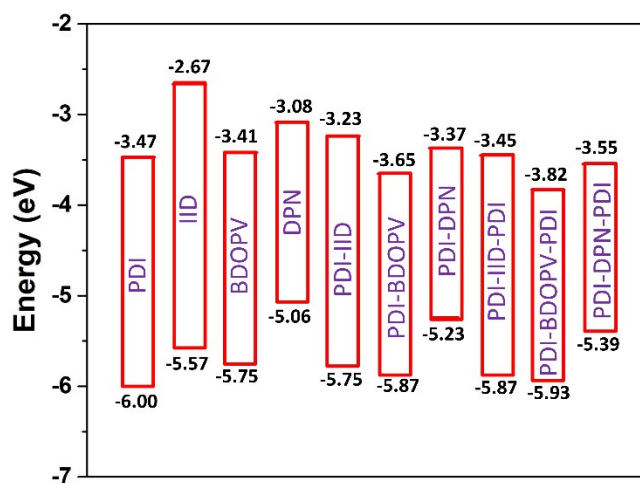


Figure S6: Calculated HOMO and LUMO energy levels of isolated **PDI**, **IID**, **BDOPV**, **DPN** and fused **PDI-IID**, **PDI-BDOPV**, **PDI-DPN**, **PDI-IID-PDI**, **PDI-BDOPV-PDI**, **PDI-DPN-PDI** molecules, calculated at B3LYP/6-31G(d,p) level of theory. All values in eV.

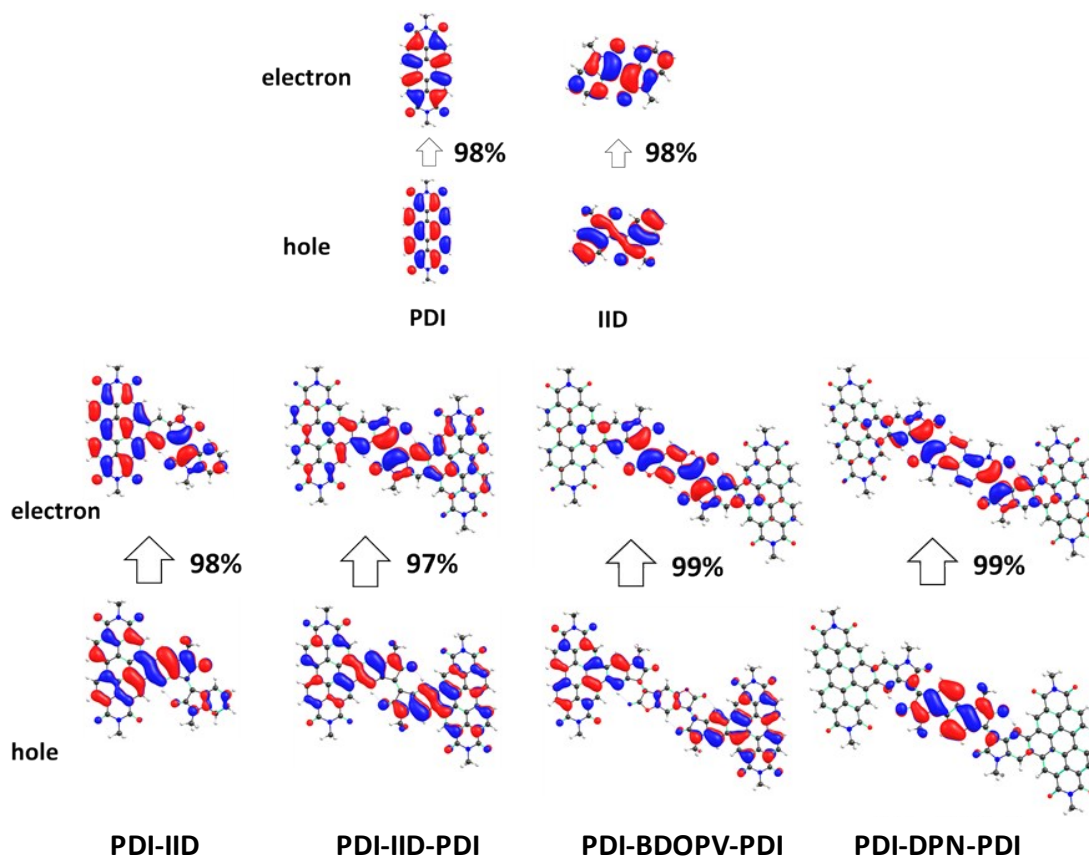


Figure S7: Pictorial representation of the natural transition orbitals (NTO) describing the $S_0 \rightarrow S_1$ transition as determined at PCM(Chloroform)-TD-OT- ω B97XD/6-

31G(d,p) level of theory; λ is the fraction of the hole-particle contribution to the excitation.

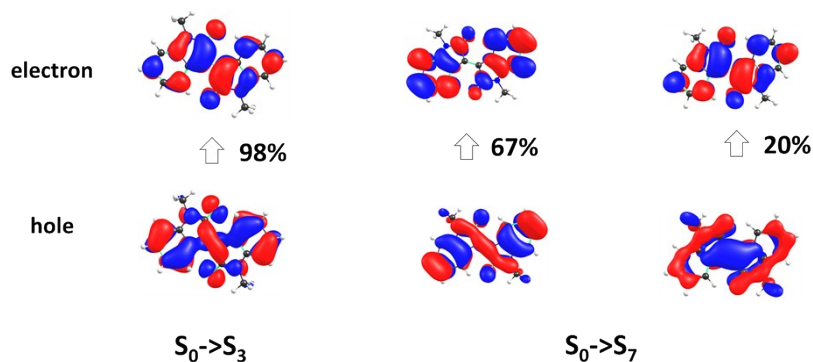


Figure S8: Pictorial representation of the natural transition orbitals (NTO) describing the $S_0 \rightarrow S_n$ transition in **IID** molecule as determined PCM(Chloroform)-TD-OT- ω B97XD/6-31G(d,p) level of theory; λ is the fraction of the hole-particle contribution to the excitation.

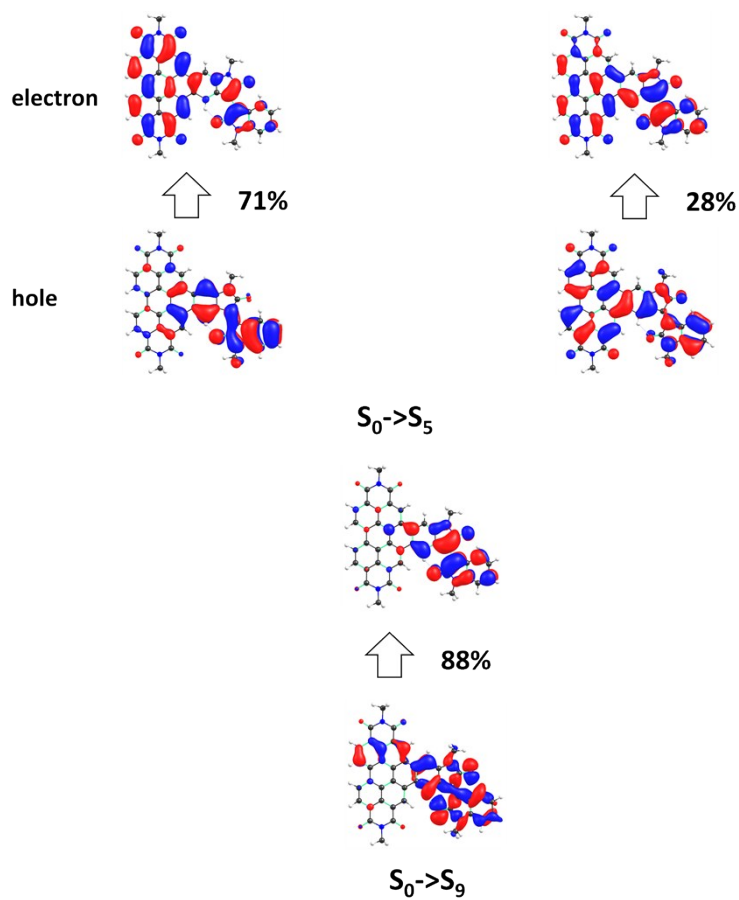


Figure S9: Pictorial representation of the natural transition orbitals (NTO) describing the $S_0 \rightarrow S_n$ transition in **PDI-IID** molecule as determined PCM(Chloroform)-TD-OT- ω B97XD/6-31G(d,p) level of theory; λ is the fraction of the hole-particle contribution to the excitation.

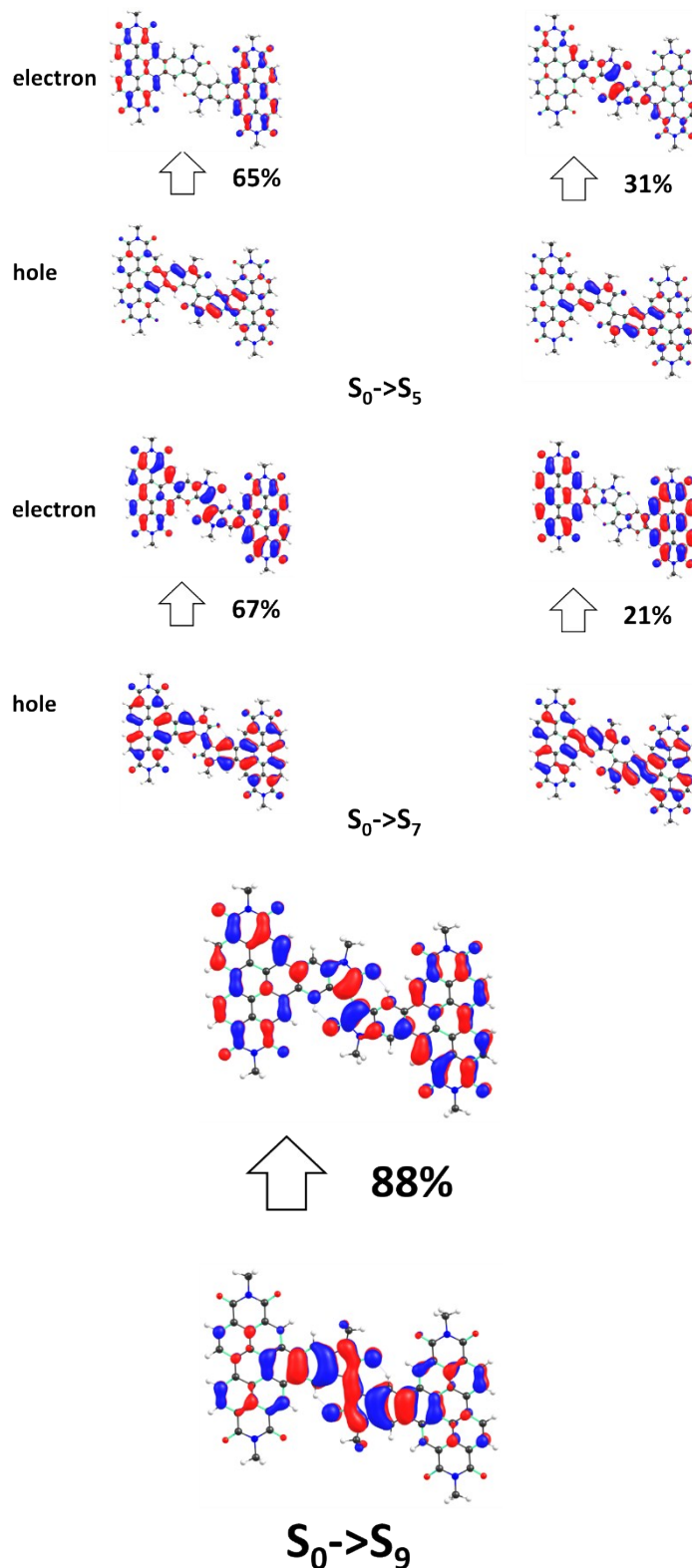


Figure S10: Pictorial representation of the natural transition orbitals (NTO) describing the $S_0 \rightarrow S_n$ transition in **PDI-IID-PDI** molecule as determined PCM(Chloroform)-TD-OT- ω B97XD/6-31G(d,p) level of theory; λ is the fraction of the hole-particle contribution to the excitation.

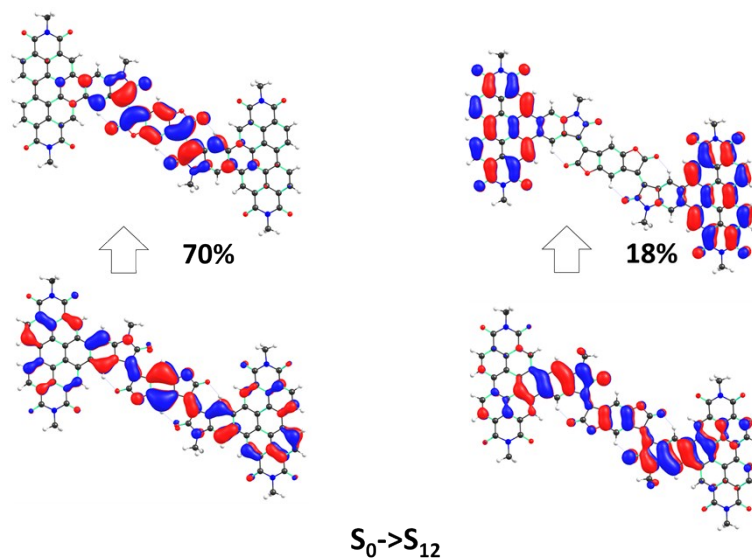


Figure S11: Pictorial representation of the natural transition orbitals (NTO) describing the $S_0 \rightarrow S_n$ transition in **PDI-BDOPV-PDI** molecule as determined PCM(Chloroform)-TD-OT- ω B97XD/6-31G(d,p) level of theory; λ is the fraction of the hole-particle contribution to the excitation.

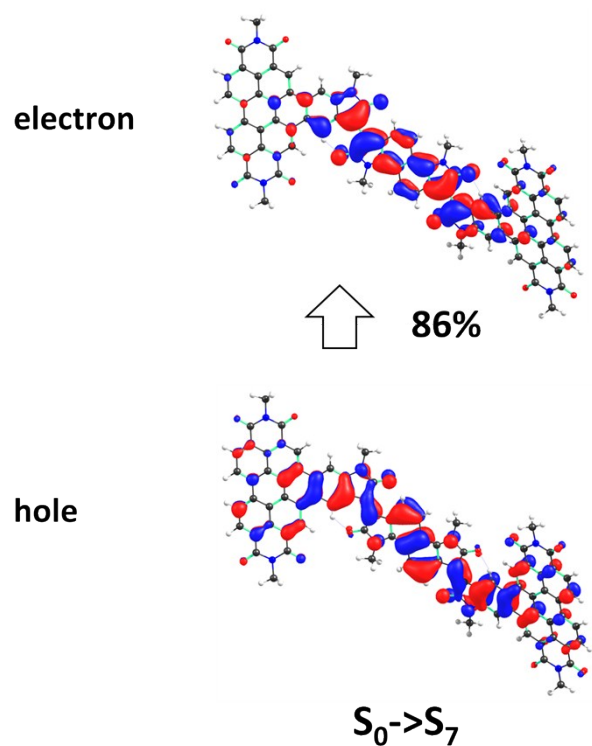


Figure S12: Pictorial representation of the natural transition orbitals (NTO) describing the $S_0 \rightarrow S_n$ transition in **PDI-DPN-PDI** molecule as determined PCM(Chloroform)-TD-OT- ω B97XD/6-31G(d,p) level of theory; λ is the fraction of the hole-particle contribution to the excitation.

3. DPVs.

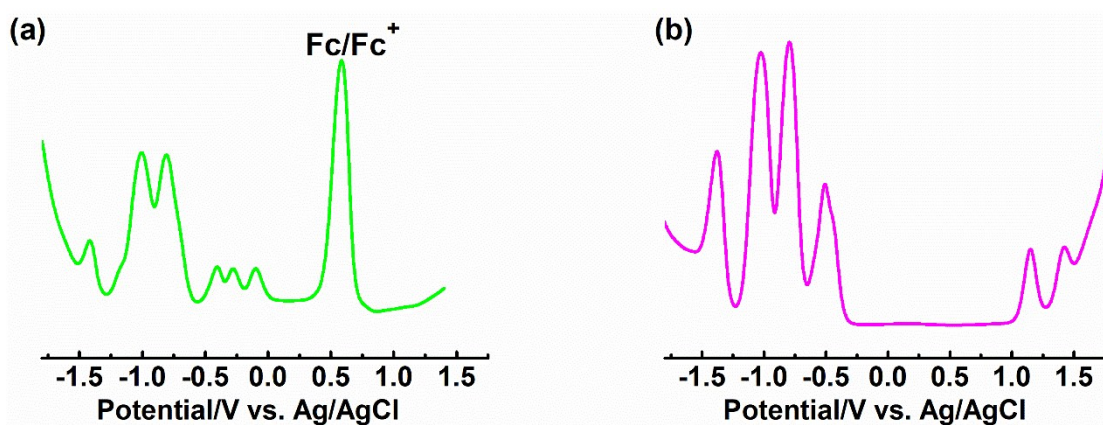


Figure S13. (a) DPV profile of compound **PDI-BDOPV-PDI**. (b) DPV profile of compound **PDI-DPN-PDI**.

4. OFET device fabrication and characterization

Table S2. The thin-film transistor properties of compounds **PDI-IID-PDI**, **PDI-BDOPV-PDI**, **PDI-DPN-PDI** in a BGBC configuration. The thin films were thermally annealed (TA) for 30 minutes before measurement and all devices were measured under nitrogen atmosphere.

Compound	Solvent	TA [°C]	μ_e [cm ² V ⁻¹ s ⁻¹]	V_T [V]	I_{on}/I_{off}
PDI-IID-PDI	chloroform	RT ^a	4.32×10^{-3}	6	3×10^4
	chloroform	60	9.14×10^{-3}	4	2×10^6
	chloroform	90	6.72×10^{-3}	2	8×10^5
	chloroform	120	6.10×10^{-3}	5	7×10^4
PDI-BDOPV-PDI	toluene	RT ^a	1.74×10^{-4}	2	1×10^5
	toluene	110	1.35×10^{-3}	44	1×10^6
	toluene	130	2.42×10^{-3}	-3	8×10^5
	toluene	150	2.37×10^{-4}	3	7×10^4
PDI-DPN-PDI	toluene	RT ^a	5.08×10^{-3}	4	1×10^4
	toluene	110	1.36×10^{-2}	8	5×10^4
	toluene	130	1.16×10^{-2}	11	1×10^5
	toluene	150	2.88×10^{-3}	22	5×10^6

^a Without thermal annealing.

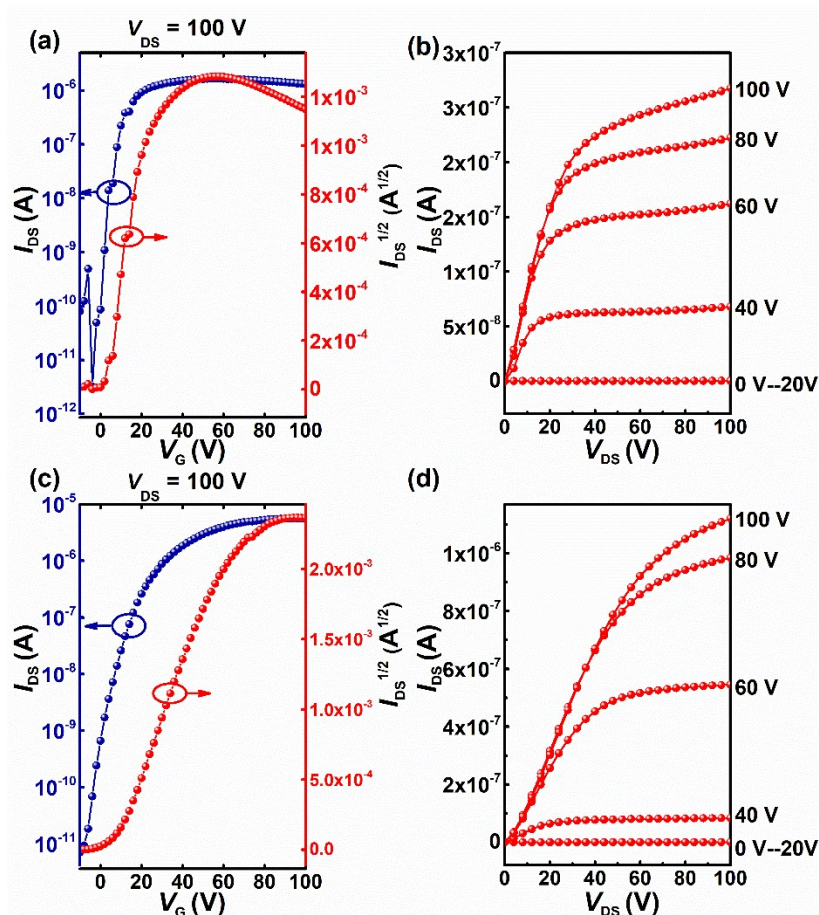


Figure S14. Transfer curves of **PDI-IID-PDI** (a), **PDI-BDOPV-PDI** (c) and output curves of **PDI-IID-PDI** (b), **PDI-BDOPV-PDI** (d) obtained from BGBC OTFT optimized devices of n-type characteristics.

Table S3. The d spacing distances of **PDI-IID**, **PDI-IID-PDI**, **PDI-BDOPV-PDI**, **PDI-DPN-PDI**. XRD was measured of the thin films at their optimized annealing temperature.

Compound	T ($^{\circ}\text{C}$) ^a	d (\AA) ^b	2θ (deg) ^c
PDI-IID	90	21.4	4.12
PDI-IID-PDI	60	-	-
PDI-BDOPV-PDI	130	22.7	3.88
PDI-DPN-PDI	110	23.1	3.82

^a Optimized annealing temperature. ^b The d spacing distances. ^c The d spacing angles

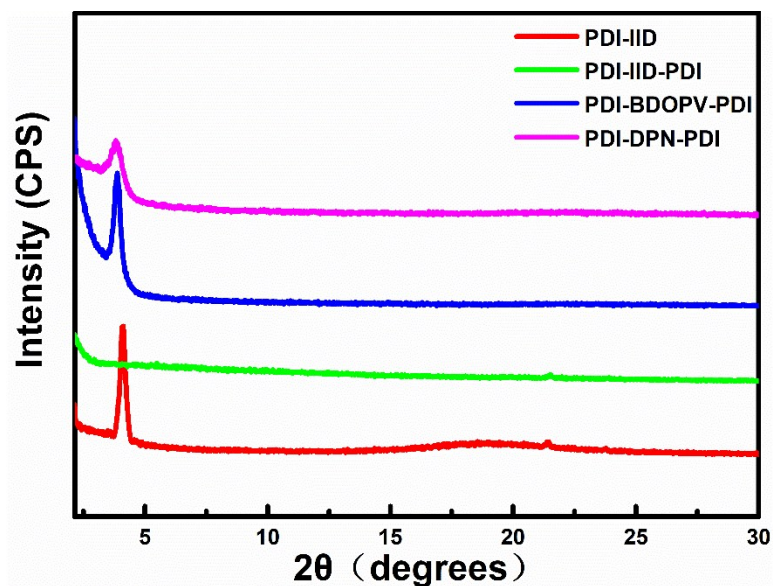


Figure S15. The XRD images of thin films of **PDI-IID**, **PDI-IID-PDI**, **PDI-BDOPV-PDI**, **PDI-DPN-PDI**.

5. Experimental details

All chemicals were purchased from commercial suppliers and used without further purification unless otherwise specified. *N*, *N'*-bis(6-undecyl)-perylene-3,4:9,10-tetracarboxylic acid diimides (**PDI**)^[1], and 1-bromo-*N*, *N'*-bis(6-undecyl)-perylene-3,4:9,10-tetracarboxylic acid diimide (**PDI-Br**)^[2] were synthesized according to the literature. octyl-6-(4,4,5,5-tetramethyl-1,3,2-dioxaborolan-2-yl) indoline-2,3-dione (**IS-B**)^[3] were synthesized according to the literature.

Compound FPDI-IS

1-octyl-6-(4,4,5,5-tetramethyl-1,3,2-dioxaborolan-2-yl)indoline-2,3-dione (**IS-B**) (206 mg, 0.53 mmol), **PDI-Br** (345.5 mg, 0.44 mmol) and $\text{Pd}_2(\text{dba})_3$ (12.2 mg, 0.013 mmol), $\text{P}(\text{t-Bu})_3\text{HBF}_4$ (15.46 mg, 0.053 mmol) were added into a glass pressure vessel under nitrogen atmosphere. Then THF (10 ml) and potassium phosphate (450 mg, 2M) were added by injection in sequence. The reaction mixture was stirred at 80°C for 12 h. The After cooling down, the mixture was poured into water, organic layer was separated with CH_2Cl_2 , dried over MgSO_4 , and purified by silica gel column chromatography (petroleum ether: CH_2Cl_2 , 1:1) to give **PDI-IS** (424 mg) which contains small quantities of **FPDI-IS** due to the easily cyclization under the natural lighting. The crude product **PDI-IS** was dissolved in CHCl_3 (200 ml) and I_2 (7 mg) was added, this solution was

subsequently exposed to sunlight at room temperature for 24 h. After removal of the solvent, the residue was purified by silica gel column chromatography (petroleum ether: CH₂Cl₂, 4:5). At last **FPDI-IS** was obtained as a red solid (254 mg, 60 %).

¹H NMR (400 MHz, 298 K, CDCl₃, ppm) δ = 9.95 (s, 1H), 9.88 (s, 1H), 9.42 (s, 1H), 9.20-9.16 (m, 2H), 9.07-9.00 (m, 2H), 8.39 (s, 1H), 5.33-5.30 (m, 2H), 4.11-4.08 (m, 2H), 2.39-2.32 (m, 4H), 2.01-1.95 (m, 6H), 1.46-1.28 (m, 34 H), 0.86-0.83 (m, 15H); ¹³C NMR (100 MHz, CDCl₃, ppm) δ = 183.9, 164.5, 159.5, 148.3, 136.8, 134.8, 133.8, 130.0, 128.7, 127.8, 127.7, 126.1, 125.1, 124.9, 124.3, 124.2, 123.3, 120.1, 103.4, 78.1, 77.8, 77.5, 56.0, 41.7, 33.3, 32.6, 32.5, 30.1, 30.0, 28.3, 27.9, 27.6, 27.5, 23.4, 14.8. HRMS (MALDI, 100%) m/z calculated for C₆₂H₇₁N₃O₆: 953.53483, found 953.53421.

Compound PDI-IID

FPDI-IS (202.7 mg, 0.21 mmol) and 1-octylindolin-2-one (53.68 mg, 0.22 mmol) was added in acetic acid (13 mL) and concentrated hydrochloric acid (1mL). The reaction mixture was stirred at 118°C for 30 h. After cooling down, the mixture was poured into water, organic layer was separated with CHCl₃, dried over MgSO₄, and purified by silica gel column chromatography (petroleum ether: CHCl₃, 2:3) to give compound **PDI-IID** as a brownish red solid (215 mg, 87%).

¹H NMR (500 MHz, 373 K, CDCl₂CDCl₂, ppm) δ = 11.30 (s, 1H), 10.16 (s, 1H), 9.93 (s, 1H), 9.31-9.29 (d, *J* = 7.8 Hz, 1H), 9.11-9.09 (m, 2H), 9.00-8.95 (m, 2H), 8.27 (s, 1H), 7.44-7.41 (t, 1H), 7.11-7.08 (t, 1H), 6.89-6.88 (d, 1H), 5.39-5.29 (m, 2H), 4.19-4.16 (t, 2H), 4.00-3.97 (t, 2H), 2.45-2.33 (m, 4H), 2.10-2.01 (m, 6H), 1.92-1.87 (m, 2H), 1.67-1.62 (m, 2H), 1.58-1.34 (m, 42H), 0.92-0.86 (m, 18H); HRMS (MALDI, 100%) m/z calculated for C₇₈H₉₂N₄O₆: 1180.70223, found 1180.70222.

Compound PDI-IID-PDI

(E)-1,1'-dioctyl-6,6'-bis(4,4,5,5-tetramethyl-1,3,2-dioxaborolan-2-yl)-[3,3'-biindolinylidene]-2,2'-dione (272 mg, 0.37 mmol) and **PDI-Br** (630 mg, 0.81 mmol), Pd₂(dba)₃ (10.12 mg, 0.011 mmol), P(t-Bu)₃·HBF₄ (12.82 mg, 0.044 mmol) were added into a glass pressure vessel under nitrogen atmosphere. Then THF (10 ml) and potassium phosphate (450 mg, 2M) were added by injection in sequence. The reaction

mixture was stirred at 80°C for 12 h. After cooling down, the mixture was poured into water, organic layer was separated with CH₂Cl₂, dried over MgSO₄, and purified by silica gel column chromatography (petroleum ether: CH₂Cl₂, 2:1) to give intermediate product (373 mg, 54 %). The intermediate product (50 mg, 0.027 mmol) was dissolved in toluene (20 ml) and I₂ (2 mg) was added, this solution was illuminated with blue light (450 nm) at 90 °C for 12 h by LED flow reactor. After removal of the solvent, the residue was purified by silica gel column chromatography (petroleum ether: CH₂Cl₂, 2:3) to give compound **PDI-III-PDI** as a deep brown red solid (32 mg, 65%).

¹H NMR (500 MHz, 373 K, CDCl₂CDCl₂, ppm) δ = 11.29 (s, 2H), 9.98 (s, 2H), 8.97 (s, 2H), 8.86-8.84 (m, 2H), 8.73-8.71 (m, 2H), 8.53-8.47 (m, 4H), 8.03 (s, 2H), 5.58-5.56 (t, 2H), 5.17-5.14 (t, 2H), 5.05 (s, 2H), 4.82 (s, 2H), 2.74 (s, 4H), 2.46-2.19 (m, 16H), 1.95-1.31 (m, 68H), 1.05-0.81 (m, 30H); HRMS (MALDI, 100%) m/z calculated for C₁₂₄H₁₄₂N₆O₆: 1875.07929, found 1875.07906.

Compound PDI-BDOPV-PDI

benzo[1,2-b:4,5-b']difuran-2,6(3H,7H)-dione (27.3 mg, 0.14 mmol), **FPDI-IS** (274 mg, 0.29 mmol) and PTSA (7.37 mg, 0.039 mmol) was degassed for three times, then added toluene (25 mL) under nitrogen atmosphere. The reaction mixture was stirred at 115°C for 24 h. After cooling down, the mixture was poured into water, organic layer was separated with CHCl₃, dried over MgSO₄, and purified by silica gel column chromatography (petroleum ether: ethyl acetate, 100:3) to give compound **PDI-BDOPV-PDI** as a purple solid (140 mg, 47 %).

¹H NMR (500 MHz, 393 K, C₆D₄Cl₂, ppm) δ = 10.40 (s, 2H), 9.40-9.29 (m, 4H), 8.95 (s, 2H), 8.68-8.67 (s, 2H), 8.35 (s, 2H), 8.10 (s, 2H), 7.85 (s, 4H), 5.46 (s, 2H), 5.26-5.20 (m, 2H), 4.44 (s, 4H), 2.64 (s, 4H), 2.43-2.22 (m, 16H), 1.85-1.16 (m, 68H) 0.93-0.87 (m, 30H); HRMS (MALDI, 100%) m/z calculated for C₁₃₄H₁₄₄N₆O₁₄: 2061.07460, found 2061.07527.

Compound PDI-DPN-PDI

3,8-didodecyl-6,8-dihydroindolo[7,6-g]indole-2,7(1H,3H)-dione (62.7 mg, 0.11

mmol), **FPDI-IS** (208 mg, 0.22mmol), P₂O₅ (10.8 mg, 0.076 mmol) and PTSA (10.4 mg, 0.055 mmol) was degassed for three times, then added toluene (25 mL) under nitrogen atmosphere. The reaction mixture was stirred at 115°C for 48 h. After cooling down, the mixture was poured into water, organic layer was separated with CHCl₃, dried over MgSO₄, and purified by silica gel column chromatography (petroleum ether: ethyl acetate, 200:7) to give compound **PDI-DPN-PDI** as a russet solid (110 mg, 41%).
¹H NMR (500 MHz, 373 K, CDCl₂CDCl₂, ppm) δ = 10.96 (s, 2H), 9.57 (s, 2H), 9.51-9.49 (m, 2H), 9.07 (s, 2H), 8.84-8.82 (s, 2H), 8.64-8.63 (m, 2H), 8.48 (s, 2H), 8.39 (s, 2H), 7.98 (s, 2H), 7.81-7.80 (d, *J* = 9.3 Hz, 2H), 5.51-5.49 (t, 2H), 5.24-5.21 (t, 2H), 4.88 (s, 2H), 4.64 (s, 2H), 4.55 (s, 2H), 4.29 (s, 2H), 2.66 (s, 4H), 2.38-2.23 (m, 16H), 1.90-1.11 (m, 108H), 1.00-0.71 (m, 36H); HRMS (MALDI, 100%) *m/z* calculated for C₁₆₂H₁₉₆N₈O₁₂: 2445.49782, found 2445.49659.

6. NMR Spectra of compounds

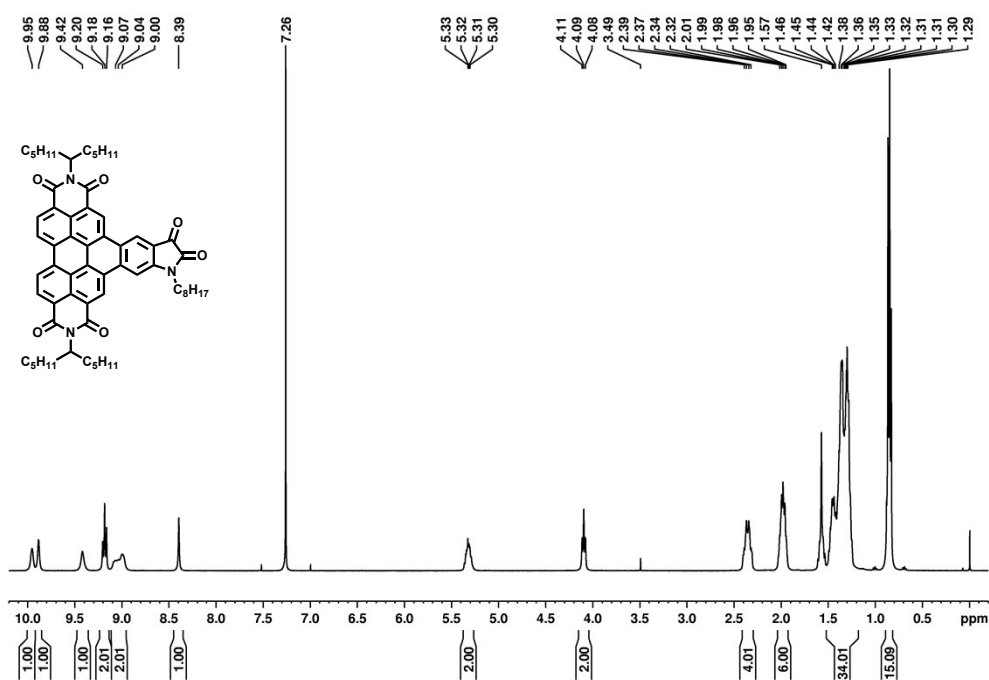


Figure S16: ¹H NMR spectrum of **FPDI-IS** in CDCl₃ at 298 K.

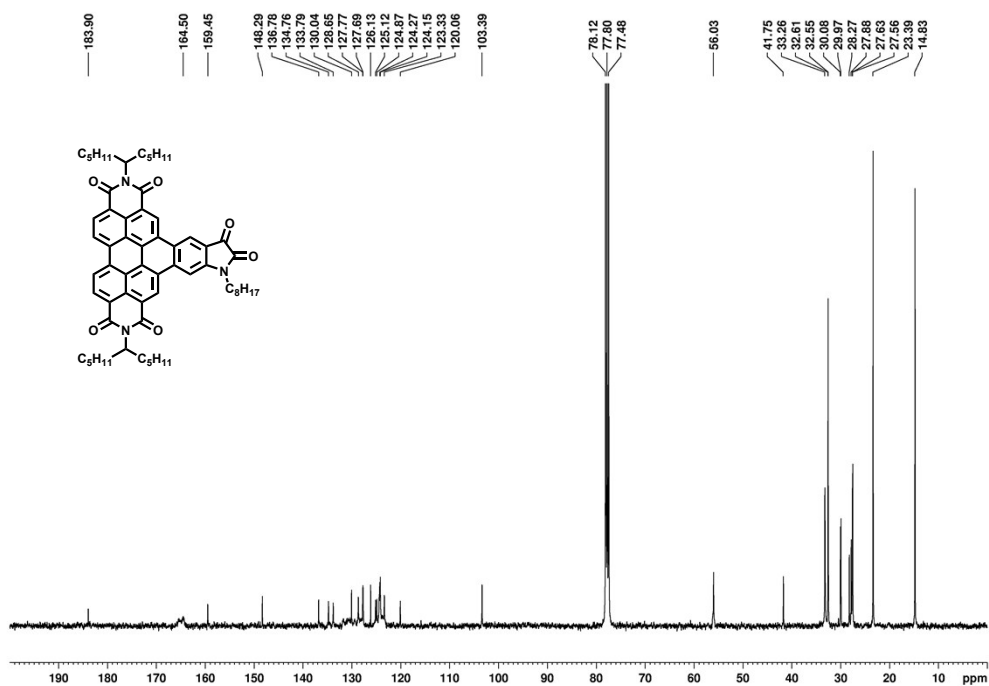


Figure S17: ^{13}C NMR spectrum of FPDI-IS in CDCl_3 at 298 K.

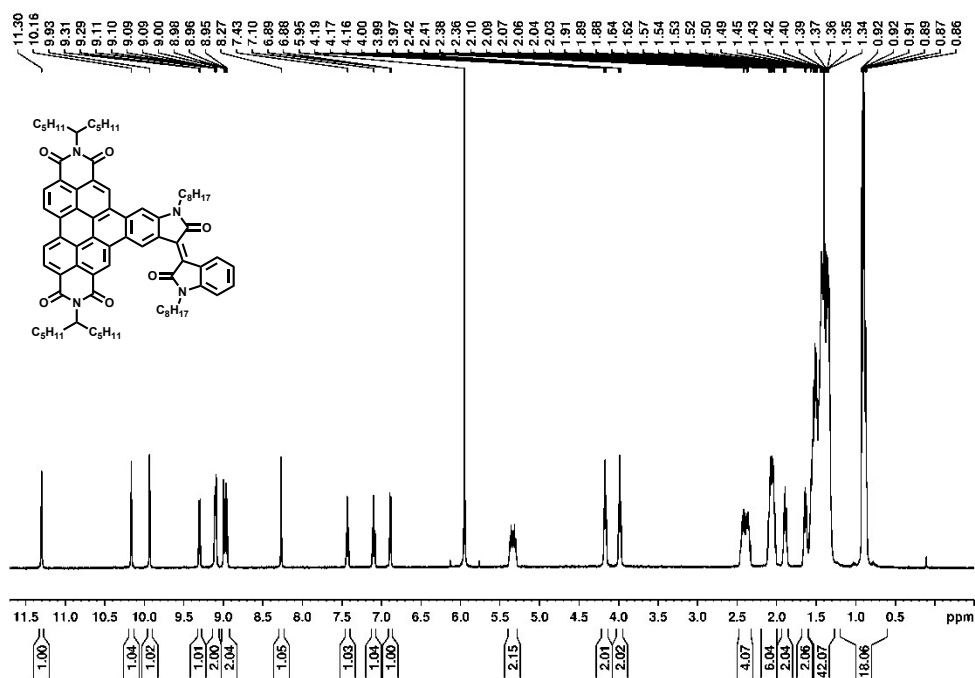


Figure S18: ^1H NMR spectrum of PDI-IID in $\text{CDCl}_2\text{CDCl}_2$ at 373 K.

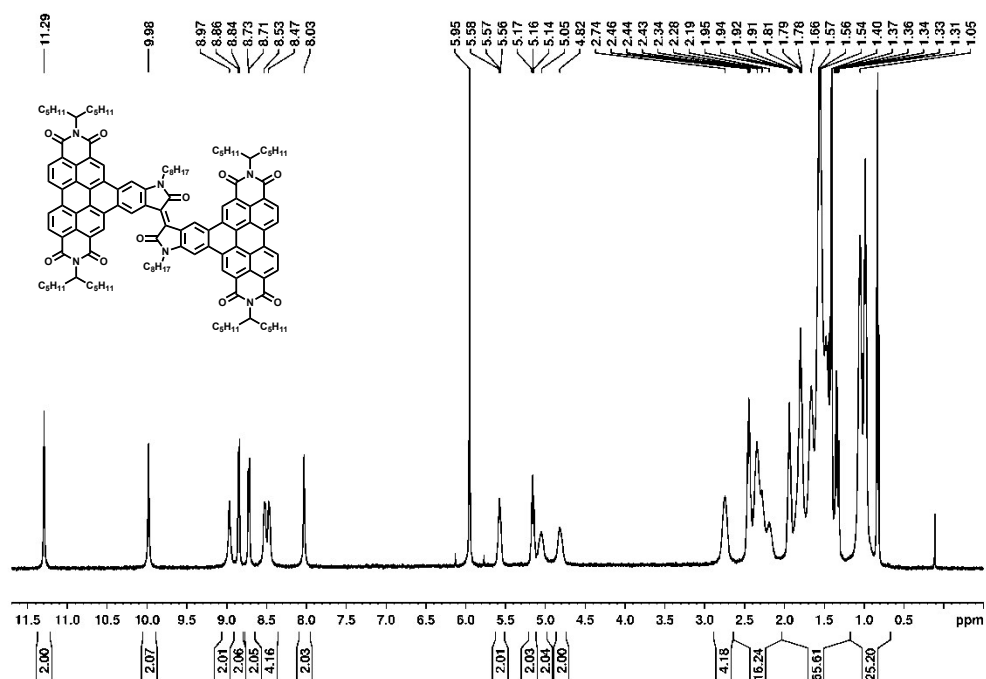


Figure S19: ¹H NMR spectrum of PDI-III-D-PDI in CDCl₂/CDCl₂ at 373 K.

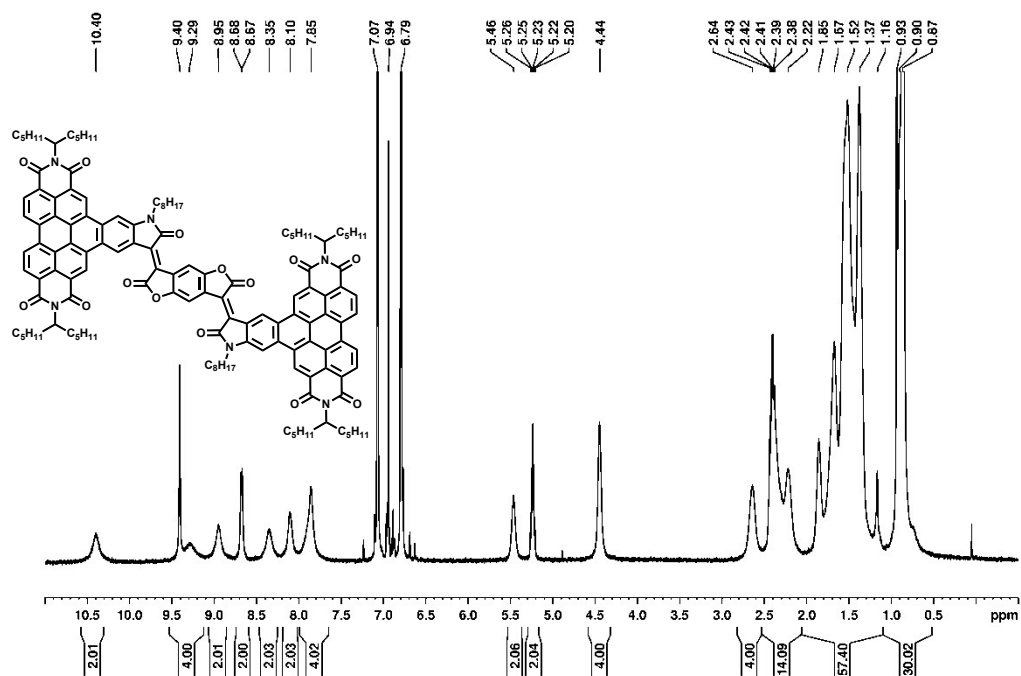


Figure S20: ¹H NMR spectrum of PDI-BDOPV-PDI in C₆D₄Cl₂ at 393 K.

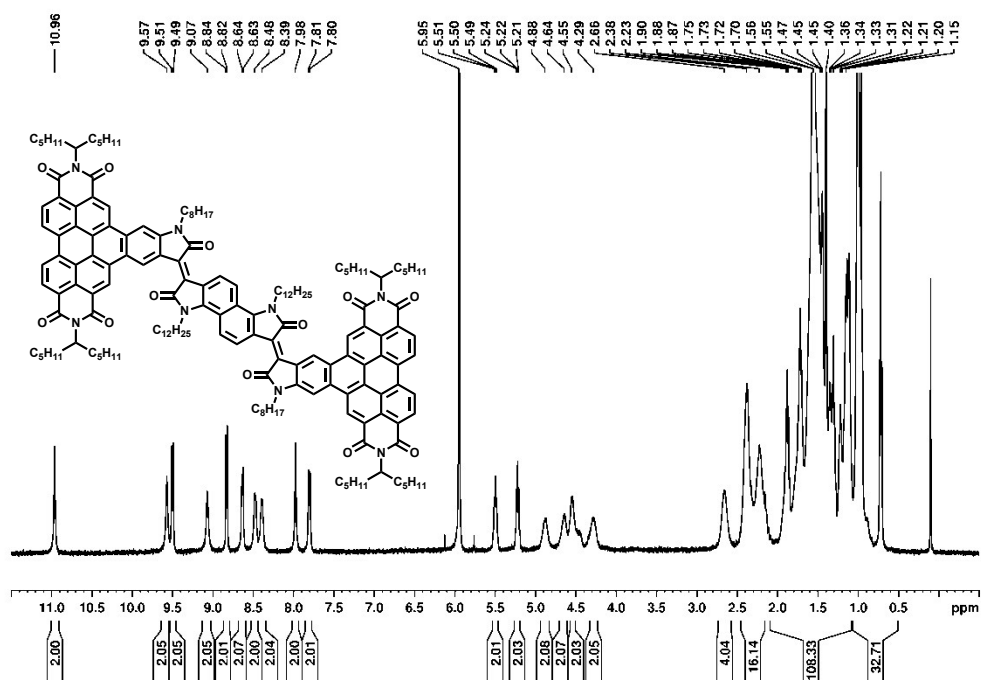
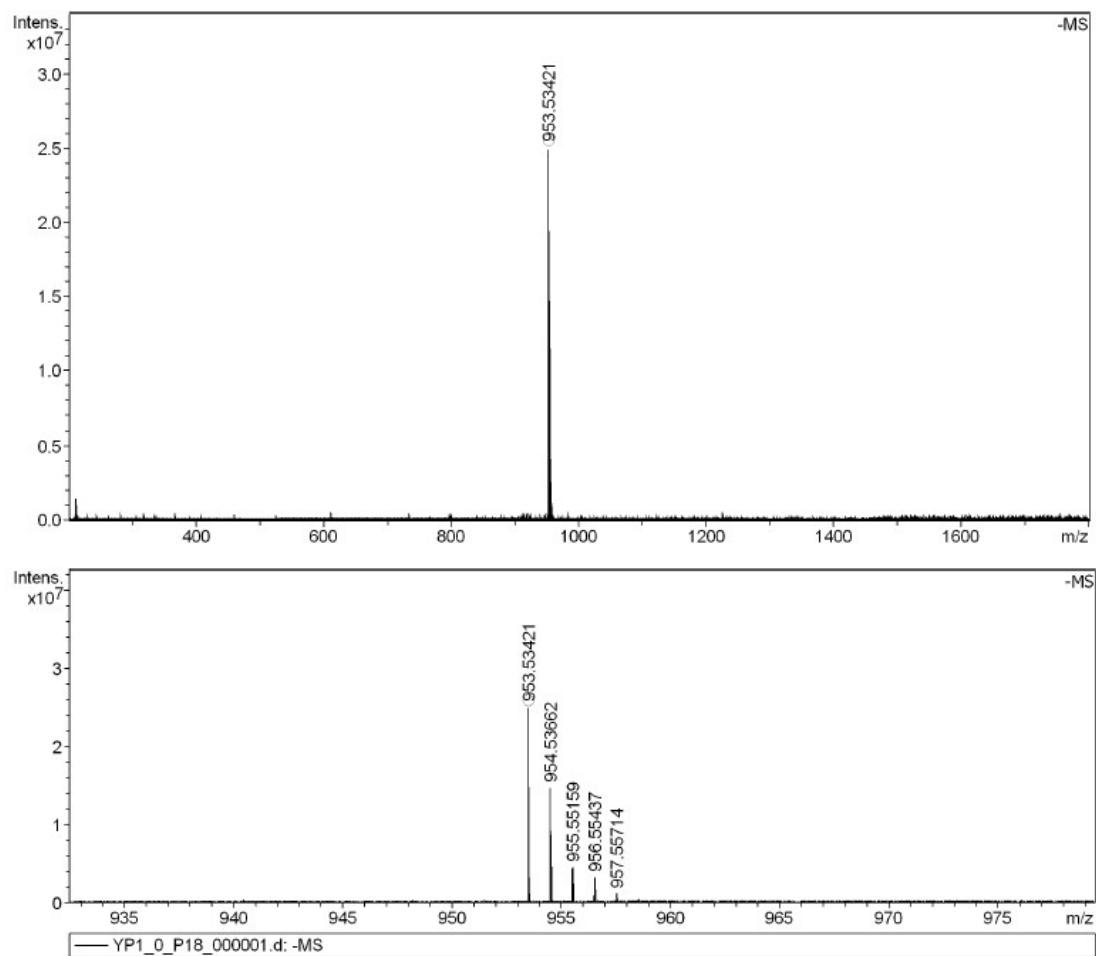


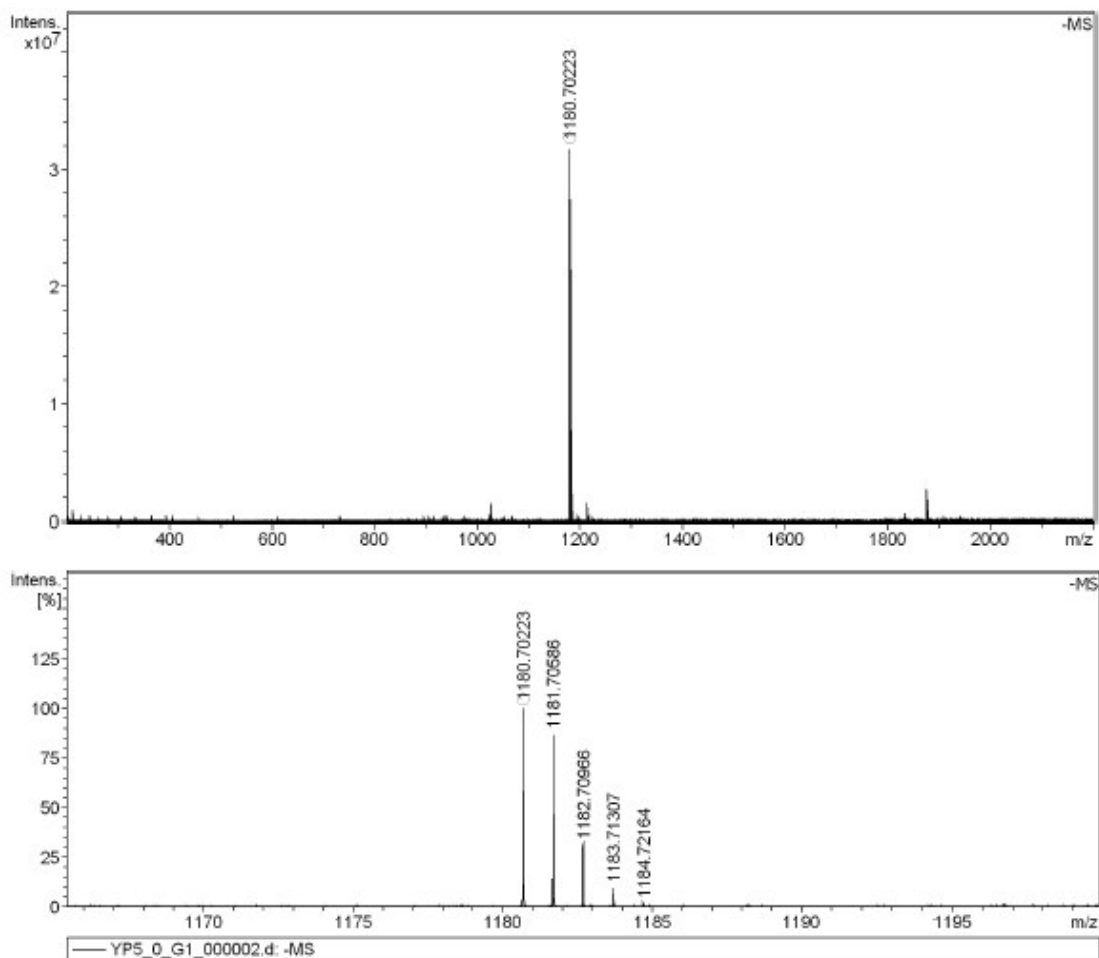
Figure S21: ^1H NMR spectrum of PDI-DPN-PDI in $\text{CDCl}_2/\text{CDCl}_2$ at 373 K.

7. HRMS spectra



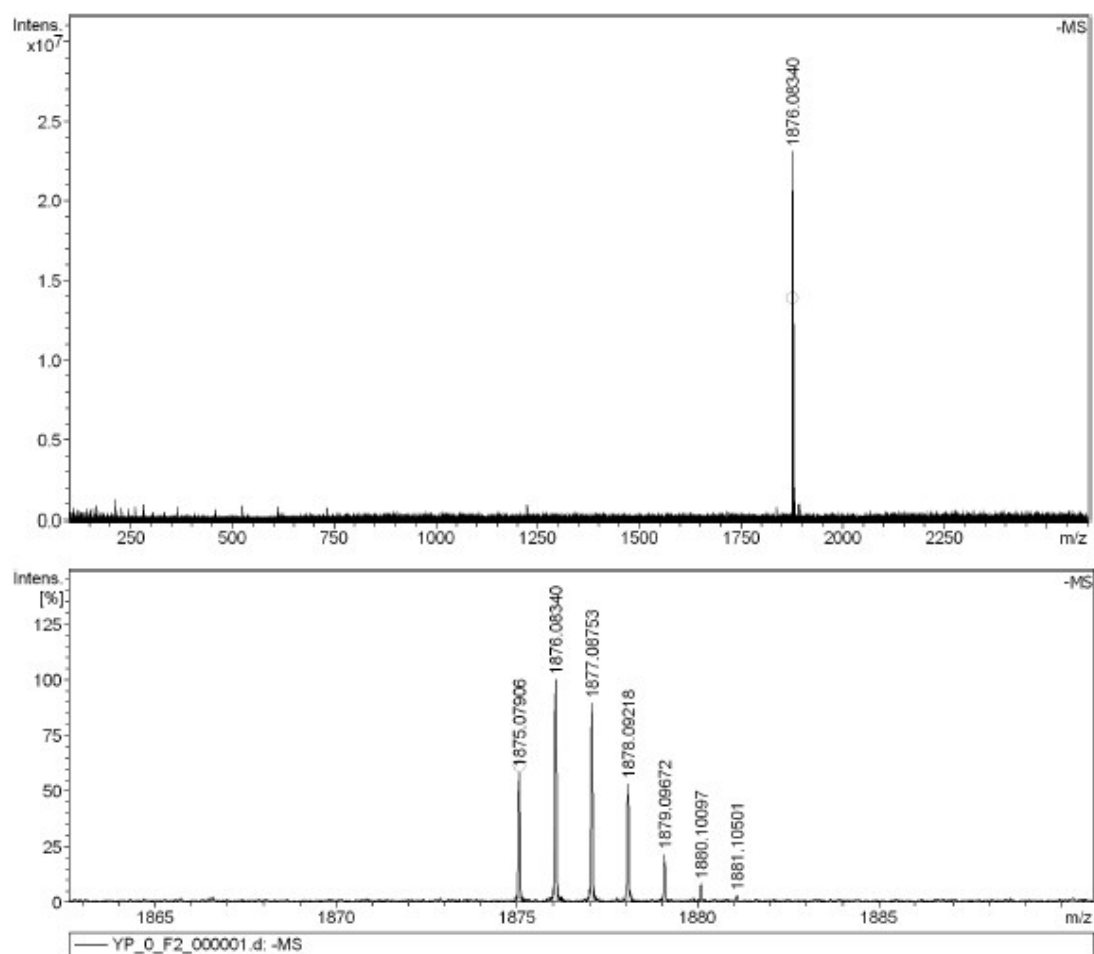
Meas. m/z	#	Ion Formula	Score	m/z	err [ppm]	Mean err [ppm]	mSigma	rdb	e ⁻ Conf	N-Rule
953.534214	1	C ₆₂ H ₇₁ N ₃ O ₆	100.00	953.534836	-0.7	1.1	56.6	29.0	odd	ok

Figure S22: HRMS spectra of FPDI-IS.



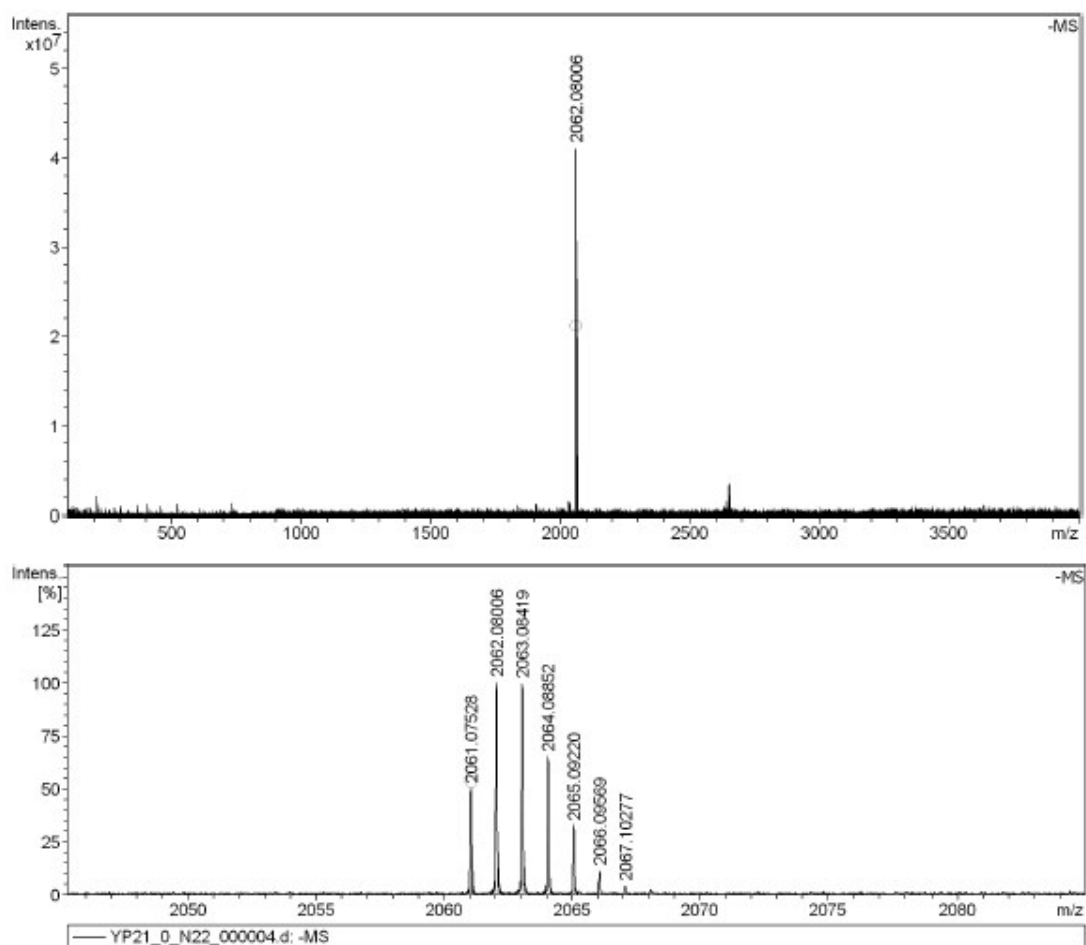
Meas. m/z	#	Ion Formula	Score	m/z	err [ppm]	Mean err [ppm]	mSigma	rdb	e ⁻ Conf	N-Rule
1180.702226	1	C78H92N4O6	100.00	1180.702235	-0.0	-0.3	35.4	35.0	odd	ok

Figure S23: HRMS spectra of PDI-III.



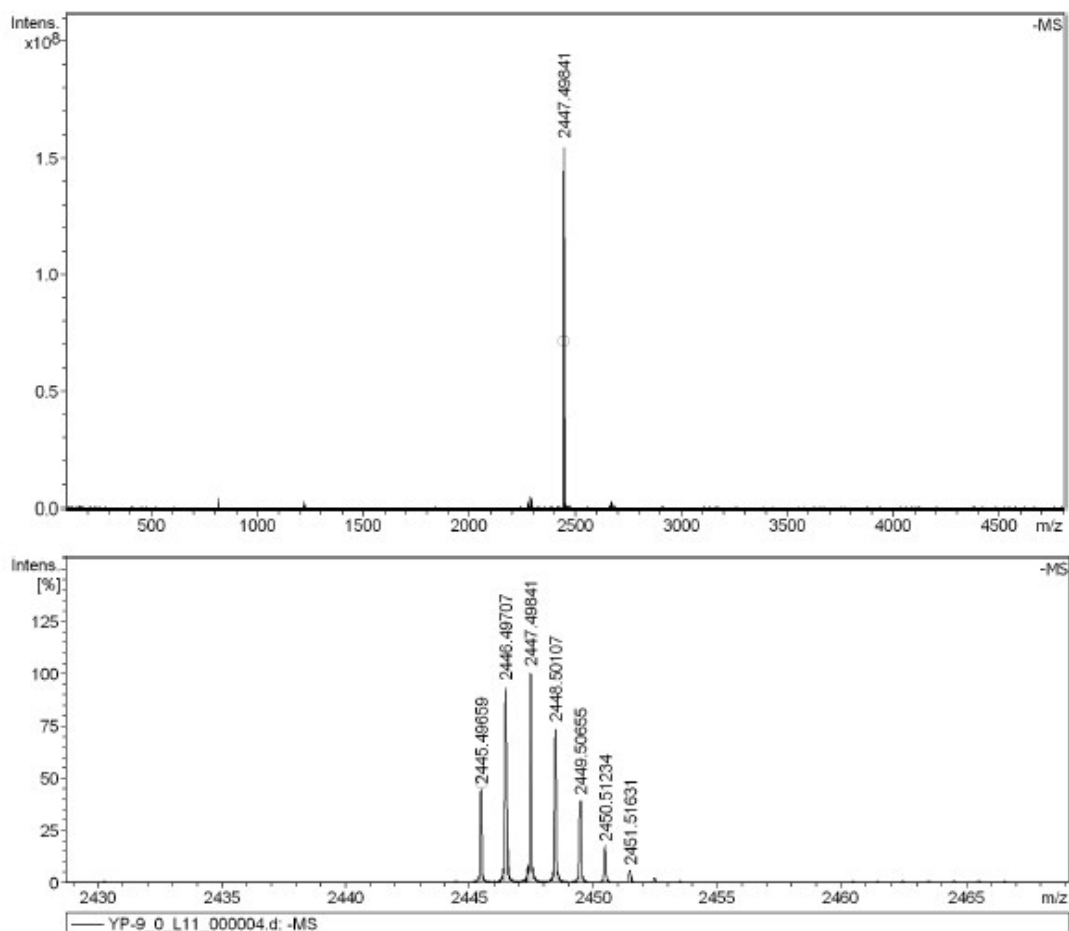
Meas. m/z	#	Ion Formula	Score	m/z	err [ppm]	Mean err [ppm]	mSigma	rdb	e ⁻ Conf	N-Rule
1875.079062	1	C ₁₂₄ H ₁₄₂ N ₆ O ₁₀	100.00	1875.079293	-0.1	-0.9	124.7	57.0	odd	ok

Figure S24: HRMS spectra of PDI-IID-PDI.



Meas. m/z	#	Ion Formula	Score	m/z	err [ppm]	Mean err [ppm]	mSigma	rdb	e ⁻ Conf	N-Rule
2061.075275	1	C134H144N6O14	100.00	2061.074602	-0.3	-1.4	162.0	66.0	odd	ok

Figure S25: HRMS spectra of PDI-BDOPV-PDI.



Meas. m/z	#	Ion Formula	Score	m/z	err [ppm]	mSigma	rdB	e ⁻ Conf	N-Rule
2445.498592	1	C162H196N8O12	100.00	2445.497822	0.5	99.5	69.0	odd	ok

Figure S26: HRMS spectra of **PDI-DPN-PDI**.

8. References:

- [1] N. V. Handa, K. D. Mendoza, L. D. Shirtcliff, *Org. Lett.* **2011**, *13*, 4724-4727.
- [2] P. Rajasingh, R. Cohen, E. Shirman, L. J. W. Shimon, B. J. Rybtchinski, *Org. Chem.* **2007**, *72*, 5973-5979.
- [3] a) H. Liao, C. Xiao, M. K. Ravva, Y. Wang, M. Little, M. V. C. Jenart, A. Onwubiko, Z. Li, Z. Wang, J.-L. Brédas, I. McCulloch, W. Yue, *Chem. Commun.* **2018**, *54*, 11152; b) N. M. Randell, C. L. Radford, J. Yang, J. Quinn, D. Hou, Y. Li, and T. L. Kelly, *Chem. Mater.* **2018**, *30*, 4864–4873.